Silencing of long non-coding RNA HRIM protects against myocardial ischemia/reperfusion injury via inhibition of NF-κB signaling

LI NIU[1], YUNQUAN ZHAO[2], SHUMEI LIU[3] and WEIWEI PAN[1]

[1]Cadre Health Department, Qingdao Municipal Hospital, Qingdao, Shandong 266011; [2]Cadre Health Department, East Hospital of Qingdao Municipal Hospital, Qingdao, Shandong 266071; [3]Cadre Health Department, West Hospital of Qingdao Municipal Hospital, Qingdao, Shandong 266005, P.R. China

Received December 25, 2019; Accepted July 17, 2020

DOI: 10.3892/mmr.2020.11597

Abstract. Myocardial ischemia/reperfusion injury (MI/RI) following cardiac surgery is a leading cause of morbidity and mortality worldwide. The aim of the present study was to investigate the role of long non-coding RNA hypoxia/reoxygenation injury-related factor in myocytes (HRIM) on cardiac function following MI/RI. After establishing an MI/RI model, hemodynamic indices were detected via transthoracic echocardiography. The proliferative and apoptotic capacities of H9C2 cells subjected to oxygen-glucose deprivation/reoxygenation were detected via Cell Counting Kit-8 assay and flow cytometry, respectively. TNF-α, IL-1β, IL-6, lactate dehydrogenase (LDH) and creatine kinase (CK) levels were measured via ELISA. The expression levels of NF-κB-associated proteins were detected via western blotting. The expression levels of HRIM were increased in the myocardial tissue of MI/RI rats and H9C2 cells. The infarct size was significantly increased following induction of MI/RI. Moreover, increased HRIM expression levels suppressed hemodynamics in MI/RI rats. Knockdown of HRIM increased cell proliferation and decreased apoptosis as well as the protein levels of phosphorylated (p)-NF-κB p65/NF-κB p65, p-IkBα/IkBα, TNF-α, IL-1β, IL-6, LDH and CK in H9C2 cells; however, these effects were attenuated via activation of NF-κB signaling. Silencing of HRIM ameliorated MI/RI injury and alleviated inflammation via inactivating the NF-κB signaling pathway.

Correspondence to: Dr Weiwei Pan, Cadre Health Department, Qingdao Municipal Hospital, 1 Jiaozhou Road, Shibei, Qingdao, Shandong 266011, P.R. China
E-mail: panweiwei220@163.com

Key words: hypoxia/reoxygenation injury-related factor in myocytes, myocardial ischemia/reperfusion injury, oxygen-glucose deprivation/reoxygenation, inflammation, NF-κB signaling pathway

Introduction

Myocardial ischemia (MI) is characterized by damage of blood vessels (1). According to the World Health Organization, ischemic heart disease has become the leading cause of human mortality worldwide (2), resulting in over 8 million deaths in 2013 (3). Although timely blood reperfusion is the most effective therapy for MI, this can lead to myocardial injury, known as myocardial ischemia/reperfusion injury (MI/RI) (4). MI/RI is associated with myocardial tissue injury, inflammation and heart failure (5-7), and is the leading cause of mortality following cardiac surgery (8). There are few effective drugs for MI/RI (9), primarily due to the poor permeability of the cytomembrane (10). Therefore, identification of novel therapeutic targets to improve the prognosis of patients with MI/RI is necessary.

Long non-coding RNAs (lncRNAs) are a class of non-coding RNA transcripts that are involved in the progression of cardiac disease. For instance, silencing of lncRNA metastasis associated lung adenocarcinoma transcript 1 (MALAT1) has been demonstrated to ameliorate acute myocardial infarction via sponging microRNA (miR)-320 (11). In addition, lncRNA 2810403D21Rik/Mirf enhances ischemia/reperfusion (I/R) injury via directly targeting miR-26a (12). Moreover, overexpression of lncRNA taurine-upregulated gene 1 promoted hypoxia-induced injury in cardiomyocytes via the miR-145-5p-Binp3 axis (13). Research has demonstrated that lncRNAs, including lncRNA urothelial carcinoma associated 1 (14), MALAT 1 (15) and hypoxia-inducible factor 1α-antisense RNA 1, are key regulators of MI/RI (16). Hypoxia/reoxygenation (H/R) injury-related factor in myocytes (HRIM; E230034O05Rik gene) is an lncRNA 1,470 bp in length located on chromosome 20p12 (including three exons) (17). Due to the upregulation of E230034O05Rik in H/R or I/R, this gene was selected for functional analysis in the present study (18). Hypoxia/reoxygenation injury-related factor in myocytes (HRIM) is co-expressed with autophagy- and apoptosis-associated proteins, including zinc finger DHHC-type palmitoyltransferase 7 (19), prostaglandin I2 synthase (20) and keratin, type I cytoskeletal 23 (21). Knockdown of HRIM has been demonstrated to increase cell

viability via mediating autophagy to protect against myocardial H/R injury (22). Consistently, silencing of HRIM has also been shown to alleviate MI/RI-induced damage (16).

NF-κB is an essential protein transcription factor involved in cell proliferation, differentiation and apoptosis (23). The NF-κB signaling pathway has been demonstrated to be associated with a number of pathological processes in the heart, including inflammation, injury and apoptosis (24). The canonical NF-κB pathway proceeds via activating the IκB kinase complex (IKK). IKK phosphorylates IκB proteins, typically IkBα, leading to dissociation from the NF-κBp65/p50 complex (25,26). The NF-κB p65/p50 complex then translocates to the nucleus, where it activates gene transcription (25,27). p65 is a major subunit of NF-κB (28). Upregulation of NF-κB p65 can enhance activation of the NF-κB signaling pathway (29), and inhibition of NF-kB p65 activity has been shown to protect against MI/RI in rats (30). Moreover, downregulation of NF-κB attenuated MI/RI in rats (31). However, whether the effects of HRIM are mediated via the NF-κB signaling pathway in MI/RI remains unclear.

The present study aimed to determine the biological function of HRIM in MI/RI rats and H9C2 cells as well as its underlying mechanism of action. These results may provide a novel target for the treatment of MI/RI.

Materials and methods

Animals. Male Sprague-Dawley rats (n=44; weight, 220-260 g; age, 7 weeks) were purchased from Beijing Vital River Laboratory Animal Technology Co., Ltd. Rats were fed standard chow and water and raised under specific pathogen-free conditions at 22˚C and 50% relative humidity with an artificial 12-h light/dark cycle. The present study was approved by the Animal Ethics Committee of Qingdao Municipal Hospital (approval no. 2020-L-054).

MI/RI model in rats. After one week of adjustment, rats were divided into Control (n=10), Sham (n=10) and MI/RI (n=24) groups. Rats without any treatment were defined as the Control group. The Sham group was subjected to all procedures except ligation. The MI/RI model was induced via ligation of the left anterior descending coronary artery (LAD) as previously described, with some modifications (30). Briefly, rats were anesthetized with pentobarbital sodium (50 mg/kg) via intraperitoneal injection. Subsequently, the LAD was ligated with a 6.0 thread and the ligation line was released after 45 min, followed by reperfusion for 24 h. Thus, an MI/RI model was established. In order to determine the effect of HRIM on MI/RI rats, MI/RI rats were divided into the following groups: MI/RI (MI/RI rats without treatment), MI/RI + small interfering RNA (siRNA) negative control (si-NC; MI/RI rats injected with 200 μg/kg/d si-NC via the tail vein following surgery) and MI/RI + HRIM siRNA (si-HRIM; MI/RI rats injected with 200 μg/kg/d si-HRIM via the tail vein following surgery) (n=8/group). Both si-NC (forward, 5'-UUCUCCGAACGUGUCACGUTT-3' and reverse, 5'-ACGUGACACGUUCGGAGAATT-3') and si-HRIM (forward, 5'-GCGCCAUUGCUGCAAAUUATT-3' and reverse, 5'-UAAUUUGCAGCAAUGGCGCTT-3') were purchased from Shanghai GenePharma Co., Ltd.

Transthoracic echocardiography (TTE). TTE was performed using a Vevo770 scanner (VisualSonics, Inc.). The left ventricular ejection fraction (LVEF), left ventricular fractional shortening (LVFS), left ventricular end-diastolic diameter (LVEDD), ventricular end-systolic diameter (LVESD), left ventricular systolic pressure (LVSP), left ventricular end-diastolic pressure (LVEDP), maximum velocity of LV contraction ($+dp/dt_{max}$) and maximum velocity of LV diastolic function ($-dp/dt_{max}$) were measured via TTE in rats.

2,3,5-Triphenyltetrazolium chloride (TTC) staining. At one week after establishment of the MI/RI model, rats were anesthetized via intraperitoneal injection of pentobarbital sodium (50 mg/kg) and sacrificed by neck dislocation. Myocardial tissue was isolated, sectioned (thickness, 3 mm), stained with 1% TTC (cat. no. A610558; Sangon Biotech Co., Ltd.) for 30 min at 37˚C, and fixed in 10% formalin for 10 min at 37˚C. After washing with water, infarct size was quantified using the Motic Med 6.0 Digital Medical Image Analysis system (Motic Instruments). Infarcted myocardium was stained white, whereas surviving myocardium was stained brick red. The infarct size was calculated as follows: Infarct size (%)=(weight of white sections/weight of whole cardiac) x100%.

Hematoxylin-eosin (HE) staining. Myocardial tissue was collected, fixed in 4% paraformaldehyde at 37˚C for 24 h, dehydrated with an ethanol gradient (70% ethanol for 2 h, 80% ethanol overnight, 90% ethanol for 2 h, 100% I ethanol for 1 h and 100% II ethanol for 1 h) vitrified with xylene, waxed, embedded in paraffin and cut into sections (thickness, 4 μm). The sections were then stained with 0.5% hematoxylin for 5 min at 37˚C, followed by 0.5% eosin for 1 min at 37˚C. The ratio of inflammatory cells/field (5 random fields) in myocardial tissues was calculated by light microscopy (magnification, x400). Stained cells were analyzed using Image-ProPlus (version 6.0; Media Cybernetics, Inc.)

Oxygen-glucose deprivation/reoxygenation (OGD/R)-induced in vitro model. MI/RI was mimicked *in vitro* by establishing an OGD/R model using myocardial cells (H9C2 cells). H9C2 cells were purchased from the Cell Bank of the Chinese Academy of Sciences and cultured in DMEM (Gibco; Thermo Fisher Scientific, Inc.) supplemented with 10% FBS at 37˚C and 5% CO_2. In order to establish an OGD/R model, serum/glucose-free DMEM was used. H9C2 cells were placed in an anaerobic chamber (95% N_2 and 5% CO_2) at 37˚C for 3 h. The medium was then replaced with normal culture medium and incubated for 0, 4 and 8 h to reoxygenate the H9C2 cells. The OGD3h/R0h, OGD3h/R4h and OGD3h/R8h groups received reoxygenation at 3 h post-OGD for 0, 4 and 8 h, respectively. In addition, H9C2 cells without treatment were regarded as the Normal group.

Cell transfection. For transfection experiments, H9C2 cells at >80% confluency were harvested and divided into three groups: OGD/R (H9C2 cells with reoxygenation at 3 h post-OGD for 8 h), OGD/R + si-NC (cells transfected with 50 nmol si-NC for 48 h) and OGD/R + si-HRIM (cells transfected with 50 nmol si-HRIM for 48 h). Asatone (an activator of the NF-κB pathway; cat. no. HY-N6826;

MedChem Express) (32) was used to further investigate the association between HRIM and the NF-κB pathway. Thus, the OGD/R + si-HRIM + Asatone group comprised cells transfected with 50 nmol si-HRIM and treated with 20 μmol/l asatone at 37˚C for 48 h. Cell transfection was performed using Lipofectamine® 3000 reagent (Invitrogen; Thermo Fisher Scientific, Inc.) at 25˚C.

Reverse transcription-quantitative PCR (RT-qPCR). Total RNA was extracted from myocardial tissue or cells using TRIzol® reagent (Invitrogen; Thermo Fisher Scientific, Inc.) and subsequently reverse-transcribed into cDNA using the PrimeScript RT reagent kit (Takara Bio, Inc.) according to the manufacturer's instructions. Subsequently, qPCR was performed using the MiScript SYBR Green PCR kit (Qiagen, Inc.) and a ABI 7500HT Fast Real-Time PCR System (Applied Biosystems; Thermo Fisher Scientific, Inc.) under the following conditions: 95˚C for 3 min and 40 cycles of 95˚C for 15 sec and 60˚C for 30 sec, and a final extension step at 72˚C for 10 min. Relative expression levels were calculated via the $2^{-\Delta\Delta Cq}$ method (33). HRIM expression levels were normalized to those of GAPDH. The primer sequences are presented in Table I.

Western blotting. A Nuclear and Cytoplasmic Protein Extraction kit (Beyotime Institute of Biotechnology) was used to extract nuclear and cytoplasmic proteins according to the manufacturer's protocol. Myocardial tissue from Sprague-Dawley rats or H9C2 cells were lysed using lysis buffer on ice to extract the total protein. Protein concentration was determined using a bicinchoninic acid protein concentration assay kit (Pierce; Thermo Fisher Scientific, Inc.). Proteins (20 μg) were separated via 10-12% SDS-PAGE and transferred onto polyvinylidene fluoride membranes. The membranes were blocked with 5% non-fat milk in Tris-buffered saline, containing 0.01% Tween-20 at 4˚C overnight. The membranes were then incubated with the following primary antibodies (all 1:1,000; all Cell Signaling Technology, Inc.) overnight at 4˚C: Anti-NF-κB p65 (cat. no. 8242), anti-phosphorylated (p)-NF-κB p65 (cat. no. 3033), anti-IκBα (cat. no. 4812) and anti-p-IκBα (cat. no. 4812), followed by incubation with horseradish peroxidase-labeled goat anti-rabbit IgG secondary antibody (1:5,000; cat. no. ab205718; Abcam) for 1 h at 37˚C. The protein bands were visualized using enhanced chemiluminescence exposure solution (Pierce; Thermo Fisher Scientific, Inc.) and quantified with Quantity One 1-D analysis software (version 4.62; Bio-Rad Laboratories, Inc.). β-actin (1:1,000; cat. no. sc-517582; Cell Signaling Technology, Inc.) was used as the internal reference.

Cell proliferation assay. Cell Counting Kit-8 (CCK-8) reagent (BD Biosciences) was used to evaluate the proliferation of H9C2 cells according to the manufacturer's instructions. H9C2 cells ($5x10^3$ cells/well) were seeded onto a 96-well plate and subjected to OGD/R. CCK-8 solution (10 μl/well) was then added and incubated for 2 h at 37˚C. The optical density at 450 nm (OD_{450}) was measured using a microplate reader (BioTek Instruments Inc.). Wells containing only culture medium and CCK-8 reagent were used as the blank group.

Table I. Primer sequences used for reverse transcription-quantitative PCR.

Name	Sequence (5'→3')
HRIM	F: AGGGGAGGGGGAAAGTAGAA
	R: CACATGGAAGCCAGTGGTCA
GAPDH	F: GACGGCCGCATCTTCTTGT
	R: CACACCGACCTTCACCATTTT

F, forward; R, reverse; HRIM, Hypoxia/reoxygenation injury-related factor in myocytes.

Flow cytometry. After 48 h transfection in 24-well plates ($3x10^5$ cells/well), cells were collected in 10 ml centrifuge tubes and centrifuged twice at 1,000 x g for 5 min at 4˚C. Subsequently, the supernatant was collected and resuspended in binding buffer (140 mM NaCl, 2.5 mM $CaCl_2$, 10 mM HEPES/NaOH, pH 7.4) to adjust the cell density to $1\text{-}5x10^6$ cells/ml. Next, 100 μl cell suspension was cultured with 5 μl V-FITC and 10 μl PI for 15 min in the dark at 25˚C. An additional 400 μl 1X binding buffer was added to each tube. The apoptotic rate was then detected using a FACSArray BD Bioanalyzer flow cytometer (BD Biosciences), and data were analyzed via CytoDiff CXP software (version 2.0; Beckman Coulter, Inc.).

ELISA. Following cell transfection, cells from each group were centrifuged at 3,000 x g at 4˚C for 10 min and the resulting supernatant was collected. The supernatant was collected and levels of TNF-α, IL-1β, IL-6, lactate dehydrogenase (LDH) and creatine kinase (CK) were measured via ELISA kits (TNF-α, cat. no. KRC3011; IL-1β, cat. no. BMS627; IL-6, cat. no. BMS625; all Thermo Fisher Scientific, Inc.; LDH, cat. no. ab183367; CK, cat. no. ab264617; both Abcam). The absorbance of each pore was measured at a wavelength of 450 nm via an enzyme mark sensing instrument (Molecular Devices LLC).

Statistical analysis. Statistical analysis was performed via SPSS software 23.0 (IBM Corp.). Data are presented as the mean ± SD of three independent repeats. Comparisons between groups were performed via ANOVA followed by post hoc Tukey's multiple comparisons test. $P<0.05$ was considered to indicate a statistically significant difference.

Results

MI/RI affects myocardial function and upregulates HRIM expression levels in rats. Once the MI/RI model was established, hemodynamic indices were evaluated via TTE. Compared with the Control and Sham groups, LVEF, LVFS, LVSP, $+dp/dt_{max}$, and $-dp/dt_{max}$ significantly decreased while LVEDD, LVESD, and LVEDP were significantly increased in the MI/RI group ($P<0.01$ and $P<0.01$; Fig. 1A). TTC staining results demonstrated that myocardial infarct size was significantly higher in the MI/RI group compared with the Sham group ($P<0.001$; Fig. 1B). HE staining revealed that

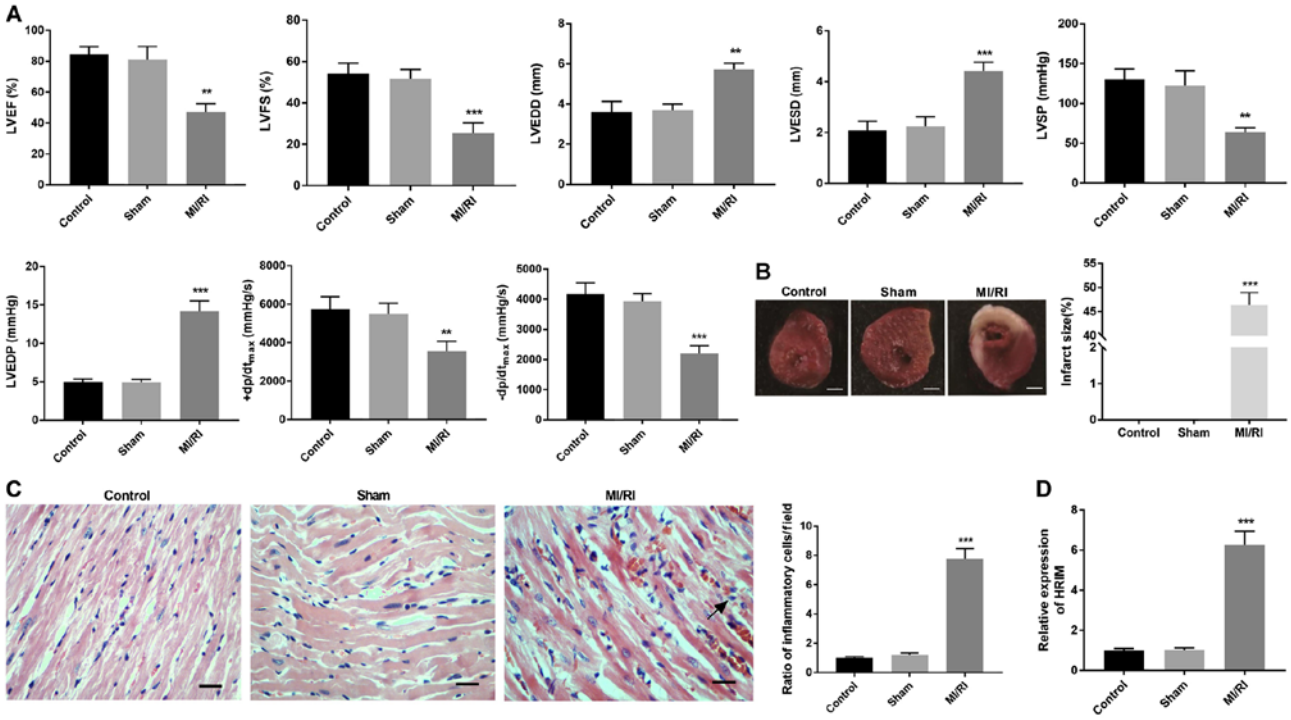

Figure 1. MI/RI affects myocardial function in rats. (A) Hemodynamics indices were evaluated via transthoracic echocardiography. (B) Myocardial infarct size was identified via 2,3,5-triphenyltetrazolium chloride staining. Scalebar, 2 mm. (C) Ratio of inflammatory cells/field in myocardial tissue was observed via hematoxylin-eosin staining. Scale bar, 100 μm. (D) Expression levels of HRIM in myocardial tissue were detected via reverse transcription-quantitative PCR. n=3. **P<0.01 and ***P<0.001 vs. Sham. MI/RI, myocardial ischemia/reperfusion injury; HRIM, hypoxia/reoxygenation injury-related factor in myocytes; LVEF, left ventricular ejection fraction; LVFS, left ventricular fractional shortening; LVEDD, left ventricular end-diastolic diameter; LVESD, ventricular end-systolic diameter; LVSP, left ventricular systolic pressure; LVEDP, left ventricular end-diastolic pressure; (+dp/dt$_{max}$, maximum velocity of LV contraction; -dp/dt$_{max}$, maximum velocity of LV diastolic function.

the ratio of inflammatory cells/field in myocardial tissue was significantly increased in the MI/RI group compared with the Sham group (P<0.001; Fig. 1C). Additionally, HRIM expression levels were significantly upregulated in the MI/RI group compared with the Sham group (P<0.001; Fig. 1D).

OGD/R induces myocardial injury and upregulates HRIM expression levels in myocardial cells. H9C2 cells were subjected to OGD/R to mimic MI/RI conditions *in vitro*. Following reoxygenation at 3 h post-OGD for 0, 4 and 8 h, the survival rate of H9C2 cells significantly decreased compared with normal cells (P<0.01 and P<0.001; Fig. 2A). RT-qPCR results demonstrated that the expression levels of HRIM in H9C2 cells significantly increased in the OGD3h/R0h, OGD3h/R4h and OGD3h/R8h groups compared with the Normal group (P<0.001; Fig. 2B). The OGD3h/R8h group was selected for subsequent experiments due to the relative high HRIM expression.

In order to examine the role of HRIM, effective HRIM knockdown was performed in H9C2 cells via si-HRIM transfection (P<0.001; Fig. 2C). The CCK-8 assay results demonstrated that the OD_{450} value of the OGD/R group was lower compared with the Normal group at 48 and 72 h post-culturing (P<0.01), and that silencing of HRIM significantly increased the OD_{450} value of H9C2 cells compared with the OGD/R + si-NC group at 48 and 72 h post-culturing (P<0.01; Fig. 2D). Additionally, apoptosis of H9C2 cells significantly increased following OGD/R compared with the Normal group (P<0.001), whereas HRIM knockdown decreased H9C2 cell apoptosis compared with the OGD/R + si-NC group (Fig. 2E).

Silencing of HRIM protects against inflammation and injury in H9C2 cells. In order to investigate the effect of HRIM knockdown on inflammation in H9C2 cells, levels of IL-1β, TNF-α and IL-6 were determined via ELISA. Compared with the Normal group, the levels of IL-1β, TNF-α and IL-6 in H9C2 cells were significantly increased in the OGD/R group (P<0.001); however, HRIM knockdown significantly attenuated these effects (P<0.001; Fig. 3A). Moreover, compared with the Normal group, the levels of LDH and CK in H9C2 cells were significantly elevated in the OGD/R group (P<0.001), and HRIM inhibition significantly decreased these levels in the OGD/R + si-HRIM group (P<0.001; Fig. 3B and C).

Silencing of HRIM inhibits the NF-κB signaling pathway. In order to evaluate the effect of HRIM inhibition on the NF-κB signaling pathway in H9C2 cells, the expression levels of NF-κB-associated proteins were measured via western blotting. The results demonstrated that the levels of p-NF-κB p65/NF-κB p65 and p-IkBα/IkBα were significantly increased in the OGD/R group compared with the Normal group (P<0.001). However, compared with the OGD/R + si-NC group, knockdown of HRIM significantly decreased the levels of p-NF-κB p65 and p-IkBα (P<0.01; Fig. 4A). Furthermore, compared with the Normal group, the levels of cytoplasmic NF-κB p65 significantly increased (P<0.001), but those of nuclear NF-κB p65 significantly decreased in the OGD/R

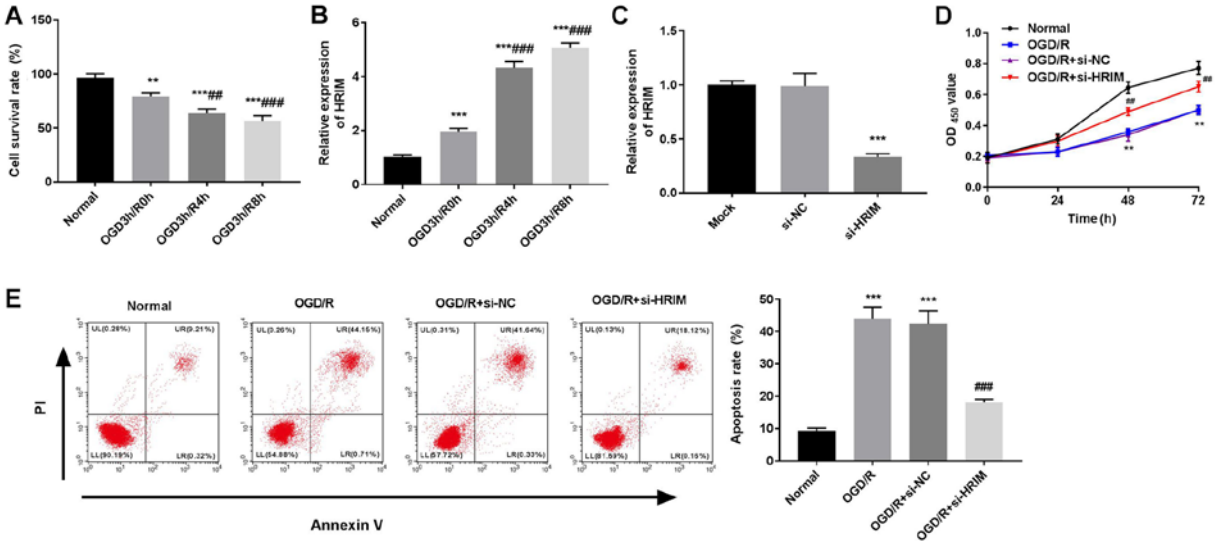

Figure 2. Silencing of HRIM enhances proliferation and attenuates apoptosis of OGD/R cells. Normal group comprised untreated H9C2 cells; OGD3h/R0h, OGD3h/R4h and OGD3h/R8h groups received reoxygenation at 3 h post-OGD for 0, 4 and 8 h, respectively. (A) Cell survival rate was assessed via CCK-8 assay. Expression levels of HRIM in (B) OGD/R and (C) transfected cells were detected via reverse transcription-quantitative PCR. **P<0.01 and ***P<0.001 vs. Normal or si-NC; $^{\#\#}$P<0.01 and $^{\#\#\#}$P<0.001 vs. OGD3h/R0h. (D) OD_{450} value at 0, 24, 48 and 72 h were observed via CCK-8 assay. (E) Apoptosis rate of H9C2 cells detected via flow cytometry. n=3. **P<0.01 and ***P<0.001 vs. Normal; $^{\#\#}$P<0.01 and $^{\#\#\#}$P<0.001 vs. OGD/R + si-NC. HRIM, hypoxia/reoxygenation injury-related factor in myocytes; OGD/R, oxygen-glucose deprivation/reoxygenation; CCK-8, Cell Counting Kit-8; OD_{450}, optical density at 450 nm; si, small interfering RNA; NC, negative control.

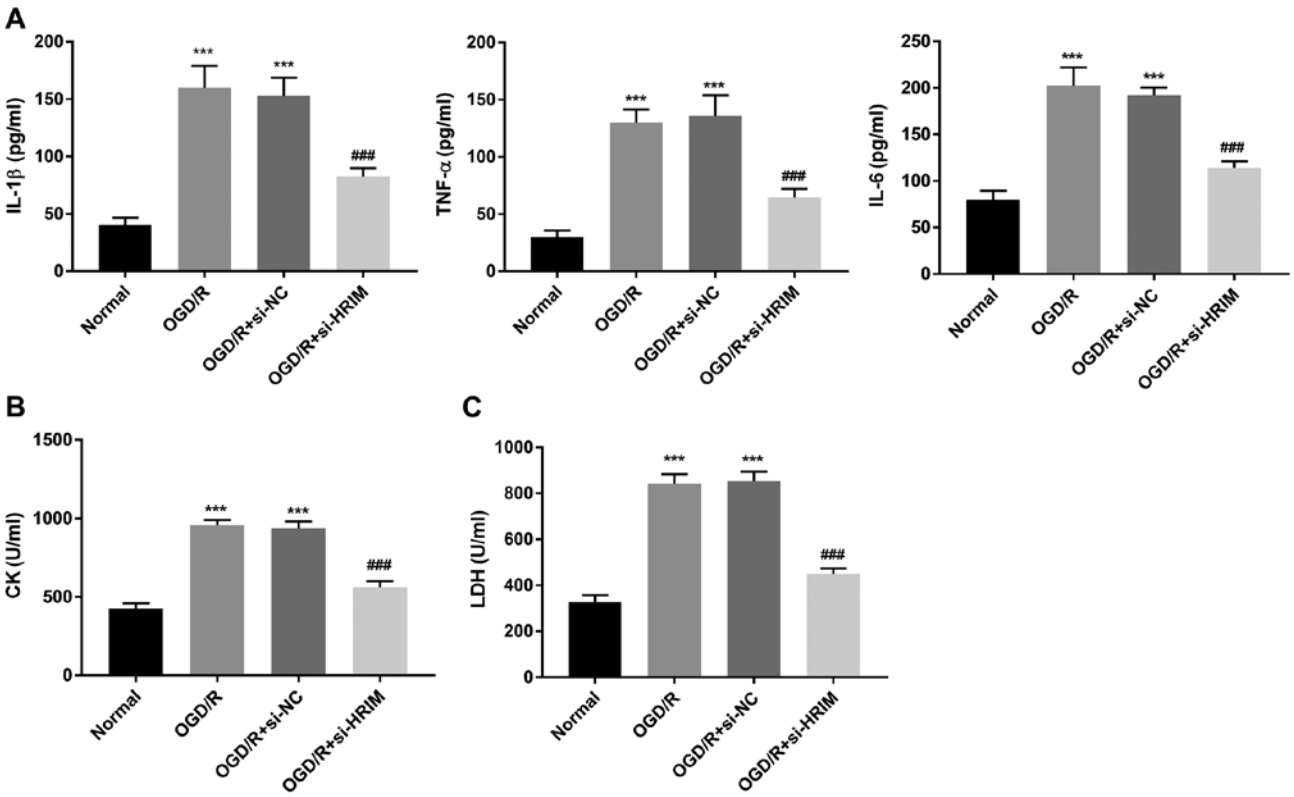

Figure 3. Silencing of HRIM protects against inflammation and injury in OGD/R cells. (A) Levels of IL-1β, TNF-α, IL-6, (B) LDH and (C) CK in H9C2 cells were measured via ELISA. n=3. ***P<0.001 vs. Normal; $^{\#\#\#}$P<0.001 vs. OGD/R + si-NC. HRIM, hypoxia/reoxygenation injury-related factor in myocytes; OGD/R, oxygen-glucose deprivation/reoxygenation; LDH, lactate dehydrogenase; CK, creatine kinase; si, small interfering RNA; NC, negative control.

group (P<0.001); however, HRIM knockdown attenuated these effects (P<0.01; Fig. 4B).

In order to investigate the association between HRIM and NF-κB signaling, H9C2 cells were treated with the NF-κB signaling pathway activator asatone. CCK-8 assay and flow cytometry results demonstrated that HRIM knockdown significantly increased the OD_{450} value at 48 and 72 h (P<0.001) post-culturing and significantly decreased the apoptosis of

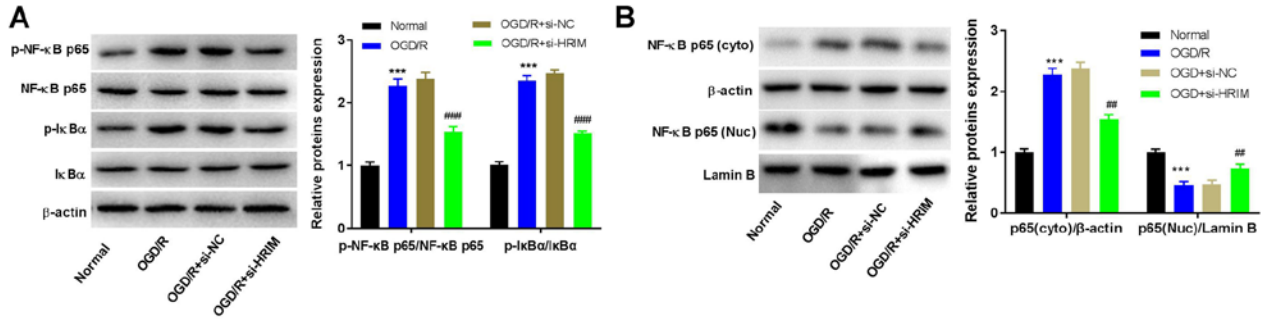

Figure 4. Silencing of HRIM inhibits the NF-κB signaling pathway in OGD/R cells. Levels of (A) p-NF-κB p65/NF-κB p65 and p-IkBα/IkBα and (B) NF-κB p65 (cyto) and (Nuc) were measured via western blotting. n=3. ***P<0.001 vs. Normal; $^{\#\#}$P<0.01, $^{\#\#\#}$P<0.001 vs. OGD/R + si-NC. HRIM, hypoxia/reoxygenation injury-related factor in myocytes; OGD/R, oxygen-glucose deprivation/reoxygenation; cyto, cytoplasmic; Nuc, nuclear; si, small interfering RNA; NC, negative control; p, phosphorylated.

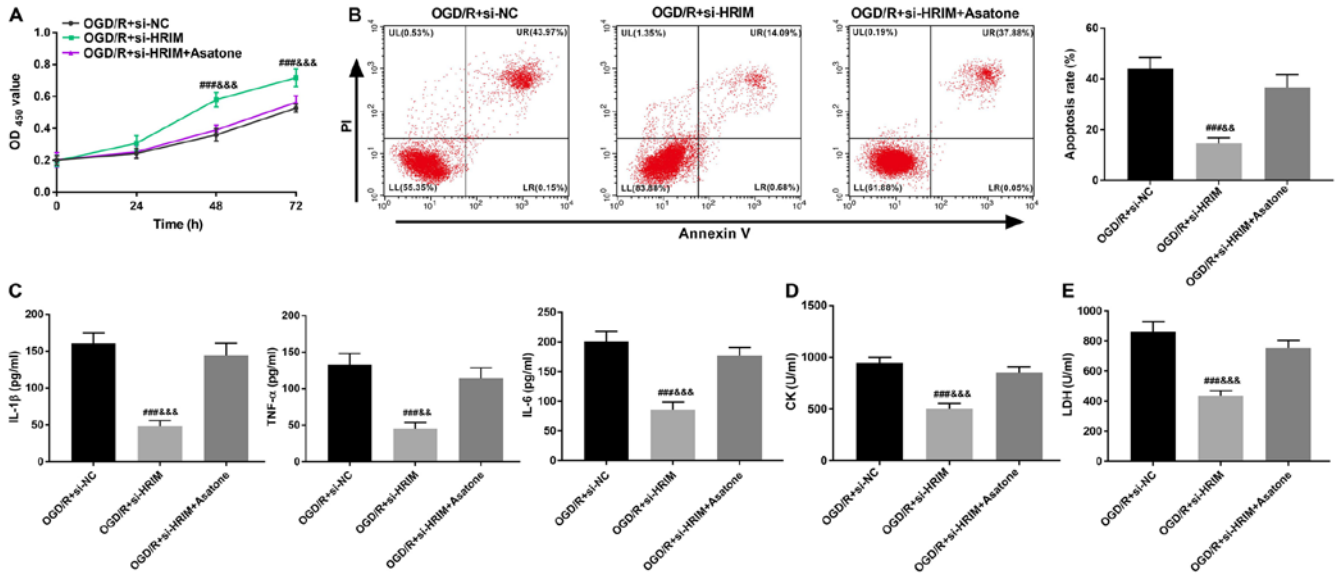

Figure 5. Silencing of HRIM regulates the NF-κB signaling pathway to alleviate injury of myocardial cells in an OGD/R model. (A) Proliferation of H9C2 cells was measured using a Cell Counting Kit-8 assay. (B) Apoptosis of H9C2 cells was detected via flow cytometry. Levels of (C) IL-1β, TNF-α, IL-6, (D) CK and (E) LDH in H9C2 cells were measured via ELISA. n=3. $^{\#\#\#}$P<0.001 vs. OGD/R + si-NC; $^{\&\&}$P<0.01 and $^{\&\&\&}$P<0.001 vs. OGD/R + si-HRIM. HRIM, hypoxia/reoxygenation injury-related factor in myocytes; OGD/R, oxygen-glucose deprivation/reoxygenation; CK, creatine kinase; LDH, lactate dehydrogenase; si, small interfering RNA; NC, negative control.

H9C2 cells (P<0.001; Fig. 5A and B). Moreover, HRIM knockdown significantly decreased the levels of TNF-α, IL-1β, IL-6, CK and LDH in H9C2 cells (P<0.001; Fig. 5C-E). However, the inhibitory effects of HRIM knockdown on H9C2 cells were reversed by treatment with asatone (P<0.01).

Silencing of HRIM inhibits MI/RI injury via inactivating the NF-κB signaling pathway. The biological function of HRIM in MI/RI rats was investigated. TTE analysis demonstrated that silencing of HRIM significantly increased the LVEF, LVFS, LVSP, +dp/dt$_{max}$ and -dp/dt$_{max}$ (P<0.05), but significantly decreased the LVEDD, LVESD and LVEDP in MI/RI rats compared with the MI/RI + si-NC group (P<0.001; Fig. 6A). Moreover, the ratio of inflammatory cells/field in myocardial tissue was significantly decreased in the MI/RI + si-HRIM group compared with that in the MI/RI + si-NC group (P<0.001; Fig. 6B). HRIM knockdown significantly decreased the expression levels of HRIM in MI/RI rats (P<0.001) compared with the MI/RI + si-NC group (Fig. 6C). Additionally, knockdown of HRIM significantly decreased the levels of p-NF-κB p65/NF-κB p65, p-IkBα/IkBα and cytoplasmic NF-κB p65 and significantly increased nuclear NF-κB p65 levels in MI/RI rats compared with the MI/RI + si-NC group (P<0.01; Fig. 6D and E).

Discussion

MI/RI is a major cause of cardiac dysfunction (34). Numerous studies have reported that abnormal expression levels of lncRNAs are associated with elevation of MI/RI (14,35). In the present study, the expression levels of HRIM in myocardial tissue of MI/RI rats were significantly upregulated, which is consistent with previously described lncRNAs (11,16). The expression levels of the lncRNAs necrosis-related factor (36), AK123487 (37) and lncRNA nuclear enriched abundant transcript 1 (38) have previously been shown to be increased

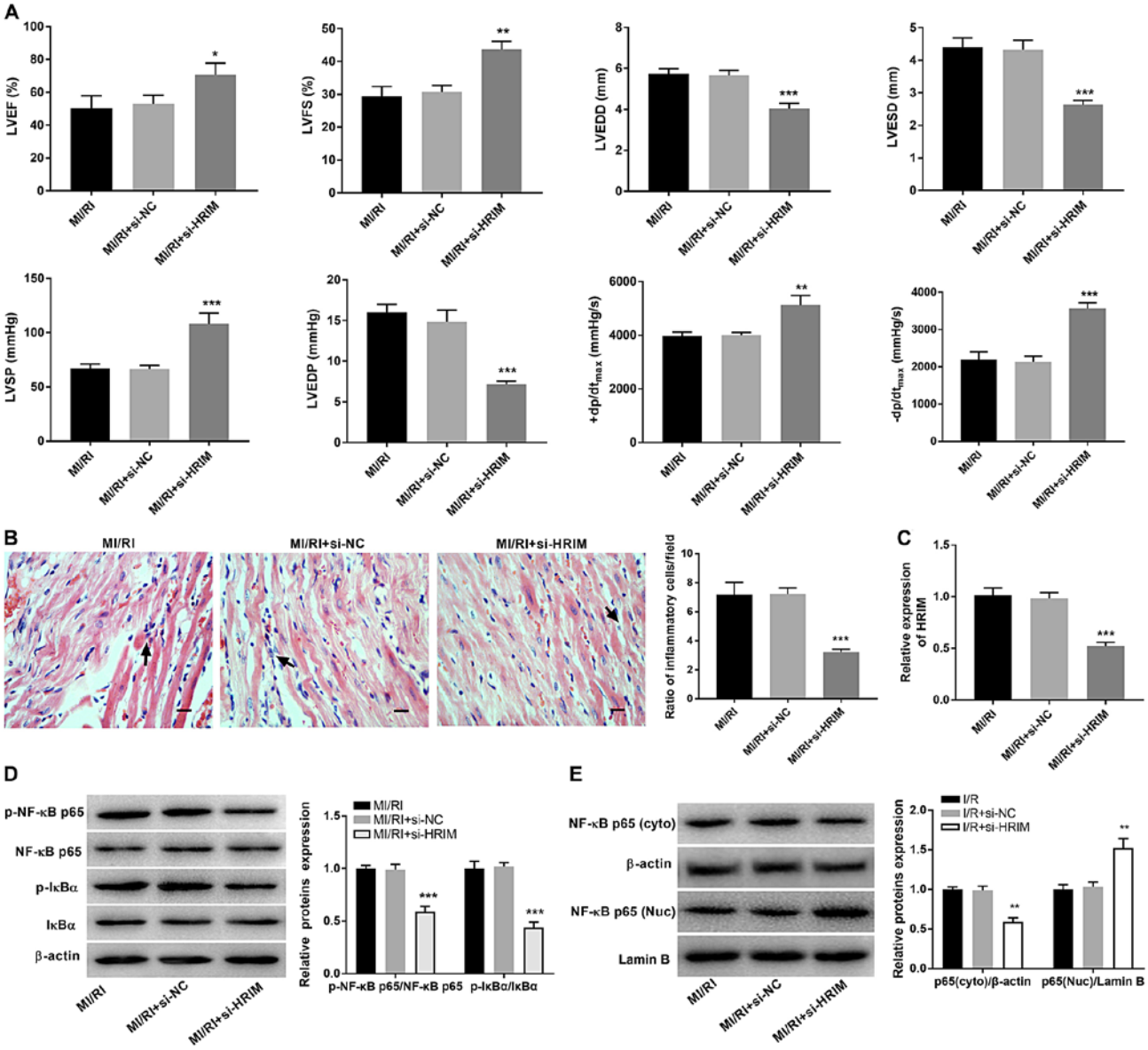

Figure 6. Silencing of HRIM attenuates MI/RI and inhibits the NF-κB signaling pathway in rats. (A) Hemodynamics indices were evaluated via transthoracic echocardiography. (B) The ratio of inflammatory cells/field in myocardial tissue was observed via hematoxylin-eosin staining. Scale bar, 100 μm. (C) Expression levels of HRIM in myocardial tissue were detected via reverse transcription-quantitative PCR. Expression levels of (D) p-NF-κB p65/NF-κB p65 and p-IkBα/IkBα and (E) NF-κB p65 (cyto) and (Nuc) were detected via western blotting. n=3. *P<0.05, **P<0.01, ***P<0.001 vs. MI/RI + si-NC. HRIM, hypoxia/reoxygenation injury-related factor in myocytes; MI/RI, myocardial ischemia/reperfusion injury; cyto, cytoplasmic; Nuc, nuclear; si, small interfering RNA; NC, negative control; LVEF, left ventricular ejection fraction; LVFS, left ventricular fractional shortening; LVEDD, left ventricular end-diastolic diameter; LVESD, ventricular end-systolic diameter; LVSP, left ventricular systolic pressure; LVEDP, left ventricular end-diastolic pressure; (+dp/dt$_{max}$, maximum velocity of LV contraction; -dp/dt$_{max}$, maximum velocity of LV diastolic function; p, phosphorylated.

in MI/RI cardiomyocytes. It was hypothesized that HRIM may serve a key role in the treatment of MI/RI. The present results demonstrated that knockdown of HRIM significantly elevated the LVEF, LVFS, LVSP, +dp/dt$_{max}$ and -dp/dt$_{max}$, and decreased the LVEDD, LVESD, LVEDP and ratio of inflammatory cells/field in myocardial tissue in MI/RI rats. Hence, these findings indicated that silencing of HRIM may improve cardiac function in MI/RI rats.

An OGD/R-induced model was established to mimic MI/RI in myocardial cells *in vitro*. Following reoxygenation at 3 h post-OGD for 0, 4 and 8 h, the survival rate of H9C2 cells was decreased, whereas HRIM expression levels were increased. A recent study has demonstrated the promoting effect of lncRNAs in the pathogenesis of cardiac diseases, including secretion of proinflammatory cytokines and myocardial cell apoptosis and damage (39). Moreover, knockdown of HRIM has been shown to increase the survival rate of H9C2 cells in H/R via decreasing autophagy in myocytes (40). Downregulation of HRIM has also been demonstrated to promote myocardial cell viability in MI/RI via inducing autophagy (41). Furthermore, inhibition of the lncRNA regulator of reprogramming has been shown to increase cell viability and decrease apoptosis in H9C2 cells (42). The present results indicated that silencing of HRIM ameliorated MI/RI in rats via increasing proliferation and decreasing apoptosis of myocardial cells. Inflammation is a key feature of MI/RI (43). Evidence has demonstrated

that inhibition of proinflammatory cytokines can ameliorate MI/RI (44,45). High levels of LDH and CK are key biomarkers of myocardial damage (46). In the present study, knockdown of HRIM significantly decreased the levels of TNF-α, IL-6, IL-1β, LDH and CK in myocardial cells. Moreover, silencing of HRIM alleviated MI/RI-induced inflammation and damage. These results indicated that HRIM knockdown may protect myocardial cells against MI/RI.

NF-κB participates in inflammatory responses and blockade of the NF-κB signaling pathway has been demonstrated to ameliorate MI/RI (47). In addition, total glucosides of peonies have been shown to alleviate MI/RI in rats via decreasing NF-κB expression levels (48). 17-methoxyl-7-h ydroxy-benzene-furanchalcone protects against MI/RI by decreasing the activity of NF-κB p65 (46). In the present study, HRIM knockdown decreased the expression levels of NF-κB-associated proteins, including p-NF-κB p65/NF-κBp65 and p-IkBα/IkBα. p65 is a major subunit of NF-κB (49). Under the action of IKK, IkBα is phosphorylated and then dissociated from the p65/p50 dimer, and p65 is dissociated in the cytoplasm (27). Phosphorylated p65 and p50 are then translocated into the nucleus (50). The phosphorylation levels of IkBα and p65 and translocation of p65 to the nucleus are key to verifying NF-κB pathway activation (51). A previous study demonstrated that silencing of the lncRNA C2dat1 inhibited focal cerebral I/R injury via suppressing the NF-κB signaling pathway (48). The present study demonstrated that silencing of HRIM suppressed NF-κB activity to alleviate MI/RI in cells, and that treatment with asatone effectively reverses this inhibitory effect. Hence, the present results indicate that silencing of HRIM may protect against MI/RI via suppression of the NF-κB signaling pathway in rats.

There are certain limitations in the present study. Due to the lack of additional data, such as clinical samples with follow-up information, it was difficult to determine the clinical importance of HRIM. Furthermore, although the NF-κB signaling pathway is regulated via HRIM, further investigation is required to determine whether HRIM is directly involved in NF-κB signaling.

In summary, the present findings demonstrated that HRIM expression levels were significantly increased in the myocardial tissue of MI/RI rats and OGD/R-induced H9C2 cells. Moreover, knockdown of HRIM decreased inflammation, apoptosis and myocardial injury via inactivating the NF-κB signaling pathway. Knockdown of HRIM also improved cardiac function in MI/RI rats. Hence, HRIM may act as a potential therapeutic target for MI/RI.

Acknowledgements

Not applicable.

Funding

No funding was received.

Availability of data and materials

The datasets used and/or analyzed during the present study are available from the corresponding author on reasonable request

Authors' contributions

LN made substantial contributions to the conception and design of the study. YZ and WP acquired the data. YZ and SL interpreted the data. SL and WP performed the experiments. SL performed the data analysis. LN and WP drafted the manuscript and revised it critically for important intellectual content. YZ revised the manuscript for critically important intellectual content. All authors read and approved the final version of the manuscript.

Ethics approval and consent to participate

This study was performed with the approval of the Animal Ethics Committee of Qingdao Municipal Hospital (approval no. 2020-L-054).

Patient consent for publication

Not applicable.

Competing interests

The authors declare that they have no competing interests.

References

1. Fröhlich GM, Meier P, White SK, Yellon DM and Hausenloy DJ: Myocardial reperfusion injury: Looking beyond primary PCI. Eur Heart J 34: 1714-1722, 2013.
2. Roger VL, Go AS, Lloyd-Jones DM, Adams RJ, Berry JD, Brown TM, Carnethon MR, Dai S, de Simone G, Ford ES, *et al*: Heart disease and stroke statistics-2011 update: A report from the American heart association. Circulation 123: e18-e209, 2011.
3. GBD 2013 Mortality and Causes of Death Collaborators: Global, regional, and national age-sex specific all-cause and cause-specific mortality for 240 causes of death, 1990-2013: A systematic analysis for the global burden of disease study 2013. Lancet 385: 117-171, 2015.
4. Zhu HJ, Wang DG, Yan J and Xu J: Up-regulation of microRNA-135a protects against myocardial ischemia/reperfusion injury by decreasing TXNIP expression in diabetic mice. Am J Transl Res 7: 2661-2671, 2015.
5. Liu NB, Wu M, Chen C, Fujino M, Huang JS, Zhu P and Li XK: Novel molecular targets participating in myocardial ischemia-reperfusion injury and cardioprotection. Cardiol Res Pract 2019: 6935147, 2019.
6. Boag SE, Andreano E and Spyridopoulos I: Lymphocyte communication in myocardial ischemia/reperfusion injury. Antioxid Redox Signal 26: 660-675, 2017.
7. Hamacher-Brady A, Brady NR and Gottlieb RA: The interplay between pro-death and pro-survival signaling pathways in myocardial ischemia/reperfusion injury: Apoptosis meets autophagy. Cardiovasc Drugs Ther 20: 445-462, 2006.
8. Niemann B, Schwarzer M and Rohrbach S: Heart and mitochondria: Pathophysiology and implications for cardiac surgeons. Thorac Cardiovasc Surg 66: 11-19, 2018.
9. Sanchez-Hernandez CD, Torres-Alarcon LA, Gonzalez-Cortes A and Peon AN: Ischemia/reperfusion injury: Pathophysiology, current clinical management, and potential preventive approaches. Mediators Inflamm 2020: 8405370, 2020.
10. Ong SB, Katwadi K, Kwek XY, Ismail NI, Chinda K, Ong SG and Hausenloy DJ: Non-coding RNAs as therapeutic targets for preventing myocardial ischemia-reperfusion injury. Expert Opin Ther Targets 22: 247-261, 2018.
11. Hu H, Wu J, Li D, Zhou J, Yu H and Ma L: Knockdown of lncRNA MALAT1 attenuates acute myocardial infarction through miR-320-Pten axis. Biomed Pharmacother 106: 738-746, 2018.
12. Liang H, Su X, Wu Q, Shan H, Lv L, Yu T, Zhao X, Sun J, Yang R, Zhang L, *et al*: LncRNA 2810403D21Rik/Mirf promotes ischemic myocardial injury by regulating autophagy through targeting Mir26a. Autophagy 16: 1077-1091, 2020.

13. Wu Z, Zhao S, Li C and Liu C: LncRNA TUG1 serves an important role in hypoxia-induced myocardial cell injury by regulating the miR1455pBinp3 axis. Mol Med Rep 17: 2422-2430, 2018.
14. Yu SY, Dong B, Zhou SH and Tang L: LncRNA UCA1 modulates cardiomyocyte apoptosis by targeting miR-143 in myocardial ischemia-reperfusion injury. Int J Cardiol 247: 31, 2017.
15. Zhao ZH, Hao W, Meng QT, Du XB, Lei SQ and Xia ZY: Long non-coding RNA MALAT1 functions as a mediator in cardioprotective effects of fentanyl in myocardial ischemia-reperfusion injury. Cell Biol Int 41: 62-70, 2017.
16. Xue X and Luo L: LncRNA HIF1A-AS1 contributes to ventricular remodeling after myocardial ischemia/reperfusion injury by adsorption of microRNA-204 to regulating SOCS2 expression. Cell Cycle 18: 2465-2480, 2019.
17. Xiong W, Qu Y, Chen H and Qian J: Insight into long noncoding RNA-miRNA-mRNA axes in myocardial ischemia-reperfusion injury: The implications for mechanism and therapy. Epigenomics 11: 1733-1748, 2019.
18. Huang Z, Ye B, Wang Z, Han J, Lin L, Shan P, Cai X and Huang W: Inhibition of LncRNA-HRIM increases cell viability by regulating autophagy levels during hypoxia/reoxygenation in myocytes. Cell Physiol Biochem 46: 1341-1351, 2018.
19. Liu ST, Chang YL, Wang WM, Chung MH, Lin WS, Chou WY and Huang SM: A non-covalent interaction between small ubiquitin-like modifier-1 and Zac1 regulates Zac1 cellular functions. Int J Biochem Cell Biol 44: 547-555, 2012.
20. Nakayama T: Genetic polymorphisms of prostacyclin synthase gene and cardiovascular disease. Int Angiol 29 (2 Suppl): S33-S42, 2010.
21. Birkenkamp-Demtroder K, Hahn SA, Mansilla F, Thorsen K, Maghnouj A, Christensen R, Øster B and Ørntoft TF: Keratin23 (KRT23) knockdown decreases proliferation and affects the DNA damage response of colon cancer cells. PLoS One 8: e73593, 2013.
22. Turkieh A, Charrier H, Dubois-Deruy E, Porouchani S, Bouvet M and Pinet F: Noncoding RNAs in cardiac autophagy following myocardial infarction. Oxid Med Cell Longev 2019: 8438650, 2019.
23. Hayden MS and Ghosh S: NF-κB, the first quarter-century: Remarkable progress and outstanding questions. Genes Dev 26: 203-234, 2012.
24. Hall G, Hasday JD and Rogers TB: Regulating the regulator: NF-kappaB signaling in heart. J Mol Cell Cardiol 41: 580-591, 2006.
25. Oeckinghaus A and Ghosh S: The NF-kappaB family of transcription factors and its regulation. Cold Spring Harb Perspect Boil 1: a000034, 2009.
26. Thomas-Jardin SE, Dahl H, Nawas AF, Bautista M and Delk NA: NF-κB signaling promotes castration-resistant prostate cancer initiation and progression. Pharmacol Ther 211: 107538, 2020.
27. Wang M, Yan S and Zhou Y: Trans-cinnamaldehyde reverses depressive-like behaviors in chronic unpredictable mild stress rats by inhibiting NF-κB/NLRP3 inflammasome pathway. Evid Based Complement Alternat Med 2020: 4572185, 2020.
28. Li Q and Verma IM: NF-kappaB regulation in the immune system. Nat Rev Immunol 2: 725-734, 2002.
29. Abd El-Mohsen M, Bayele H, Kuhnle G, Gibson G, Debnam E, Kaila Srai S, Rice-Evans C and Spencer JP: Distribution of [3H] trans-resveratrol in rat tissues following oral administration. Br J Nutr 96: 62-70, 2006.
30. Liang X, Huang J, Lin X, Qin F, Wen Q, Chen C, Li Y, Ge W and Huang R: The effect of 17-methoxyl-7-hydroxy-benzene-fu ranchalcone on NF-κB and the inflammatory response during myocardial ischemia reperfusion injury in rats. J Cardiovasc Pharmacol 63: 68-75, 2014.
31. Lu L, Wei P, Cao Y, Zhang Q, Liu M, Liu XD, Wang ZL and Zhang PY: Effect of total peony glucoside pretreatment on NF-κB and ICAM-1 expression in myocardial tissue of rat with myocardial ischemia-reperfusion injury. Genet Mol Res 15: 2016.
32. Chang HY, Chen YC, Lin JG, Lin IH, Huang HF, Yeh CC, Chen JJ and Huang GJ: Asatone prevents acute lung injury by reducing expressions of NF-[Formula: See text]B, MAPK and inflammatory cytokines. Am J Chin Med 46: 651-671, 2018.
33. Livak KJ and Schmittgen TD: Analysis of relative gene expression data using real-time quantitative PCR and the 2(-Delta Delta C(T)) method. Methods 25: 402-408, 2001.
34. Yang Y, Duan W, Jin Z, Yi W, Yan J, Zhang S, Wang N, Liang Z, Li Y, Chen W, *et al*: JAK2/STAT3 activation by melatonin attenuates the mitochondrial oxidative damage induced by myocardial ischemia/reperfusion injury. J Pineal Res 55: 275-286, 2013.
35. Chen J, Hu Q, Zhang BF, Liu XP, Yang S and Jiang H: Long noncoding RNA UCA1 inhibits ischaemia/reperfusion injury induced cardiomyocytes apoptosis via suppression of endoplasmic reticulum stress. Genes Genomics 41: 803-810, 2019.
36. Wang K, Liu F, Liu CY, An T, Zhang J, Zhou LY, Wang M, Dong YH, Li N, Gao JN, *et al*: The long noncoding RNA NRF regulates programmed necrosis and myocardial injury during ischemia and reperfusion by targeting miR-873. Cell Death Differ 23: 1394-1405, 2016.
37. Zheng C, Wu Z, Tian L, Li D, Wang X, He Y, He Y, Jin W, Li M, Zhu Q, *et al*: Long noncoding RNA AK12348 is involved in the regulation of myocardial ischaemia-reperfusion injury by targeting PARP and caspase-3. Heart Lung Circ 27: e51-e58, 2018.
38. Luo M, Sun Q, Zhao H, Tao J and Yan D: Long noncoding RNA NEAT1 sponges miR-495-3p to enhance myocardial ischemia-reperfusion injury via MAPK6 activation. J Cell Physiol 235: 105-113, 2020.
39. Yang F, Qin Y, Wang Y, Li A, Lv J, Sun X, Che H, Han T, Meng S, Bai Y and Wang L: LncRNA KCNQ1OT1 mediates pyroptosis in diabetic cardiomyopathy. Cell Physiol Biochem 50: 1230-1244, 2018.
40. Xie XJ, Fan DM, Xi K, Chen YW, Qi PW, Li QH, Fang L and Ma LG: Suppression of microRNA-135b-5p protects against myocardial ischemia/reperfusion injury by activating JAK2/STAT3 signaling pathway in mice during sevoflurane anesthesia. Biosci Rep 37: BSR20170186, 2017.
41. Hu X, Dai S, Wu WJ, Tan W, Zhu X, Mu J, Guo Y, Bolli R and Rokosh G: Stromal cell derived factor-1 alpha confers protection against myocardial ischemia/reperfusion injury: Role of the cardiac stromal cell derived factor-1 alpha CXCR4 axis. Circulation 116: 654-663, 2007.
42. Zhang W, Li Y and Wang P: Long non-coding RNA-ROR aggravates myocardial ischemia/reperfusion injury. Braz J Med Biol Res 51: e6555, 2018.
43. Hausenloy DJ and Yellon DM: Myocardial ischemia-reperfusion injury: A neglected therapeutic target. J Clin Invest 123: 92-100, 2013.
44. Shin IW, Jang IS, Lee SM, Park KE, Ok SH, Sohn JT, Lee HK and Chung YK: Myocardial protective effect by ulinastatin via an anti-inflammatory response after regional ischemia/reperfusion injury in an in vivo rat heart model. Korean J Anesthesiol 61: 499-505, 2011.
45. Hadi NR, Alamran F, Yousif M and Zamil ST: Antiapoptotic effect of simvastatin ameliorates myocardial ischemia/reperfusion injury. ISRN Pharmacol 2013: 815094, 2013.
46. Hu X, Cui B, Zhou X, Xu C, Lu Z and Jiang H: Ethyl pyruvate reduces myocardial ischemia and reperfusion injury by inhibiting high mobility group box 1 protein in rats. Mol Biol Rep 39: 227-231, 2012.
47. He XH, Wang Y, Yan XT, Wang YL, Wang CY, Zhang ZZ, Li H and Jiang HX: Transduction of PEP-1-heme oxygenase-1 fusion protein reduces myocardial ischemia/reperfusion injury in rats. J Cardiovasc Pharmacol 62: 436-442, 2013.
48. Xu Q, Deng F, Xing Z, Wu Z, Cen B, Xu S, Zhao Z, Nepomuceno R, Bhuiyan MIH, Sun D, *et al*: Long non-coding RNA C2dat1 regulates CaMKIIdelta expression to promote neuronal survival through the NF-κB signaling pathway following cerebral ischemia. Cell Death Dis 7: e2173, 2016.
49. Wu M, Gu J, Mei S, Xu D, Jing Y, Yao Q, Chen M, Yang M, Chen S, Yang B, *et al*: Resveratrol delays polycystic kidney disease progression through attenuation of nuclear factor κB-induced inflammation. Nephrol Dial Transplant 31: 1826-1834, 2016.
50. Tian F, Zang WD, Hou WH, Liu HT and Xue LX: Nuclear factor-kB signaling pathway constitutively activated in esophageal squamous cell carcinoma cell lines and inhibition of growth of cells by small interfering RNA. Acta Biochim Biophys Sin (Shanghai) 38: 318-326, 2006.
51. Krappmann D and Vincendeau M: Mechanisms of NF-κB deregulation in lymphoid malignancies. Semin Cancer Biol 39: 3-14, 2016.